PHYSICAL REVIEW C VOLUME 26, NUMBER 3 SEPTEMBER 1982

# Pion-nucleon scattering in the $P_{11}$ channel

S. Morioka* and I. R. Afnan
*School of Physical Sciences, The Flinders University of South Australia, Bedford Park, South Australia 5042, Australia*
(Received 13 August 1981)

We present a parametrization of the $\pi$-$N$ interaction in the $P_{11}$ channel in which the amplitude is the sum of a pole part and a non-pole part ($t=t_{\rm pole}+t_{\rm np}$) and satisfies two-body unitarity. Here $t_{\rm pole}$ has both the nucleon propagator and the $\pi NN$ vertex dressed. The final amplitude fits the scattering length and low energy $\pi$-$N$ phase shifts ($T_\pi^{\rm lab}<300$ MeV). We study the effect of a resonance in $t_{\rm np}$ on the phase shifts, $\pi NN$ coupling constant, and the off-shell behavior of the amplitude.

[NUCLEAR REACTIONS $\pi N$ scattering in $P_{11}$ channel, renormalization, resonance effect.]

## I. INTRODUCTION

Recent investigations into the inclusion of the effect of real pion absorption in $\pi$-$d$ elastic scattering,[1,2] and its extension to pion-nucleus scattering,[3,4] have required the splitting of the $\pi$-$N$ amplitude in the $P_{11}$ channel into a pole part and a non-pole part, i.e.,

$$t=t_{\rm pole}+t_{\rm np}=fgf^{+}+t_{\rm np}\ . \qquad (1)$$

In this way the non-pole part ($t_{\rm np}$) gives rise to pion multiple scattering, while the pole part ($t_{\rm pole}$) gives the coupling to the pion absorption channel. In Eq. (1) the pole part of the amplitude, which is separable, is given in terms of the dressed nucleon propagator $g$, and the dressed $\pi NN$ vertex $f$. This structure for the $\pi$-$N$ interaction is quite different from that commonly used in $\pi$-$d$ elastic scattering, and in the construction of pion-nucleus optical potential,[5] where the $\pi$-$N$ amplitude has no nucleon pole. Experimentally the $\pi$-$N$ phase shifts in the $P_{11}$ channel are small at low energies. This has been used to justify the fact that the contribution of the $P_{11}$ amplitude to $\pi$-$d$ scattering is small and can be neglected.[6] However, the fact that $t$ is the sum of a repulsive contribution ($t_{\rm pole}$) and an attractive contribution ($t_{\rm np}$), which contribute differently to $\pi$-$d$ and possibly $\pi$-$A$ scattering, can make the total effect of the $P_{11}$ channel important. Furthermore, the $P_{11}$ amplitude has the $N^*(1470)$ resonance which should, if included, lead to a modification of the $\pi NN$ vertex $f$ through the dressing, and again can lead to significant effect in $\pi$-$d$ elastic scattering and pion absorption.

The aim of the present investigation is to construct a $P_{11}$ amplitude of the form given in Eq. (1) with the full dressing for both the nucleon propagator and the $\pi NN$ vertex. In this way we can:

(i) Compare our amplitudes with those[7] derived from a potential.

(ii) Investigate the effect of a resonance in $t_{\rm np}$ on the $\pi$-$N$ phase shifts and $\pi NN$ vertex.

In Sec. II we present our basic equations which are derived using the diagrammatic method developed by Taylor[8] for quantum field theory. For the sake of future application of these amplitudes in $\pi NN$ calculations, we assume $t_{\rm np}$ to be separable (i.e., they are the solution of the two-body equation for a separable potential). We then proceed in Sec. III to a discussion of mass and wave function renormalization in our model. Here we find that our wave function renormalization $Z_2>0$, indicating the absence of ghost poles. In Sec. IV we present and discuss our numerical results. We find that in the absence of a resonance pole our amplitudes are similar to those[7] obtained from a two term separable potential. However, the inclusion of an $N^*(1470)$ resonance pole does affect the off-shell behavior of the $\pi$-$N$ amplitude and can have some influence on the $\pi$-$d$ elastic cross section.

## II. THE BASIC EQUATIONS

The derivations of the basic equations were presented elsewhere.[9–11] Here we give a brief diagrammatic presentation and the corresponding algebraic expressions. Using Taylor's classification[8] of the diagrams that contribute to the $\pi$-$N$ amplitude by exposing intermediate states, and restricting ourselves to including two-body unitarity only, we get the set of equations given diagrammatically in Figs. 1(a)–1(c). The corresponding alegbraic expressions are

$$t = t^{(1)} + f^{(1)} g f^{(1)+} , \tag{2}$$

$$t^{(1)} = t^{(2)} + t^{(2)} G t^{(1)} , \tag{3}$$

$$f^{(1)} = f^{(2)} + t^{(1)} G f^{(2)} , \tag{4}$$

where $t$ is the full $\pi$-$N$ amplitude and $f$ is the $\pi NN$ vertex. The number in parentheses is the maximum irreducibility of the amplitude or vertex. For example, $t^{(2)}$ includes all amplitudes that are one- and two-particle irreducible. The one- and two-particle dressed propagators are denoted by $g$ and $G$, respectively, and are represented in Figs. 1(a)–1(d) by a line with a dot. The first and second terms in Eq. (2) correspond to $t_{\mathrm{np}}$ and $t_{\mathrm{pole}}$ in Eq. (1), respectively. Furthermore, if $t^{(2)}$ is taken to be a "potential" then Eq. (3) reduces to the standard two-body equation except that $G$ is fully dressed at this stage. This dressing in $G$ can be reduced to a simple mass renormalization if we are to neglect three-body unitarity. The one-particle propagator $g$ is also dressed; however, its dressing contributes to two-body unitarity and cannot be neglected. We can

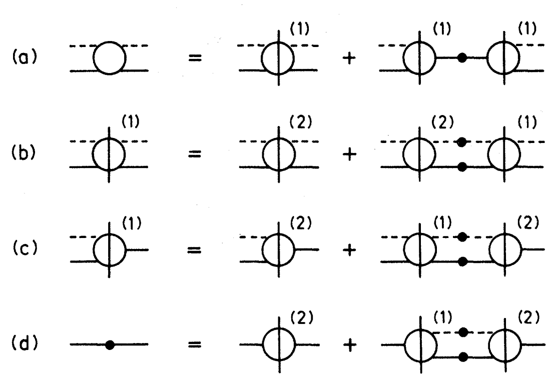


FIG. 1. Classification of the diagrams for the $\pi$-$N$ amplitude.

write the dressed one-particle propagator in terms of the bare propagator $g_0$ as

$$g = (g_0^{-1} - \Sigma^{(1)})^{-1} , \tag{5}$$

where the self-energy term $\Sigma^{(1)}$ is given by [see Fig. 1(d)]

$$\Sigma^{(1)} = \Sigma^{(2)} + f^{(1)+} G f^{(2)} . \tag{6}$$

These results were originally derived[8] within the framework of a covariant quantum field theory, and the decomposition of the two-particle irreducible diagrams in Eqs. (2)–(4), and (6) may be carried on by exposing three- and more particle intermediate states. However, since we do not intend to include three or more particle unitarity explicitly into our equations, we will assume that $\Sigma^{(2)}$, $f^{(2)}$, and $t^{(2)}$ are independent of the total energy. In this way our final amplitude satisfies two-body unitarity but does not include the threshold for pion production (i.e., three-body unitarity).

Since it is common practice[12] in pion-nucleus scattering to treat the pion relativistically while the nucleons are treated nonrelativistically, we take for our propagators

$$g_0(E) = (E - m_N)^{-1} , \tag{7}$$

$$G(E) = G_0(E) = [E - E(p)]^{-1} , \tag{8}$$

with

$$E(p) = \sqrt{p^2 + m_\pi^2} + m_N + \frac{p^2}{2m_N} . \tag{9}$$

Here $E$, $m_N$, $m_\pi$, and $p$ are the total energy, the physical nucleon and pion masses, and the relative momentum of the $\pi$-$N$ system in the center of mass.

Since we hope to use our $\pi$-$N$ interaction in a three-body type $\pi NN$ calculation, it is advantageous to have a $\pi$-$N$ interaction that is separable. To see if one can justify approximating the potential $t^{(2)}$ by a separable potential, let us consider the physical content of $t^{(2)}$. According to our diagrammatic classification $t^{(2)}$ is the class of all $\pi N \rightarrow \pi N$ diagrams with at least two pions in every intermediate state. The lowest order contribution to this class is the diagram in Fig. 2. Note the appearance of this

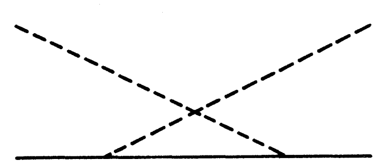

FIG. 2. The lowest order diagram of $t^{(2)}$.

diagram in $t^{(2)}$ rather than the pole amplitude is the result of using time ordered diagrams which in turn result from the use of Blankenbecler-Sugar reduction or the use of nonrelativistic kinematics. This lowest order diagram can be approximated by a separable potential.[13] Although the higher order diagrams are by no means separable, we will approximate $t^{(2)}$ by a separable potential for the practical purpose of using it in many-body calculation. Furthermore, this gives us the added advantage of being able to introduce resonances in $t_{\text{np}}=t^{(1)}$ most simply. We therefore define

$$t^{(2)}=|h\rangle\lambda\langle h| \ , \tag{10}$$

where $\lambda=+1\ (-1)$ corresponding to a repulsive (attractive) interaction. We now can write Eqs. (2)–(4), (6), and (7) as

$$t(E)=|h\rangle\tau(E)\langle h| + |f^{(1)}(E)\rangle g(E)\langle f^{(1)}(E)| \ , \tag{11}$$

$$|f^{(1)}(E)\rangle=|f^{(2)}\rangle + |h\rangle\tau(E)\langle h|G_0(E)|f^{(2)}\rangle \ , \tag{12}$$

$$\tau(E)=(\lambda^{-1}-\langle h|G_0(E)|h\rangle)^{-1} \ , \tag{13}$$

$$g(E)=[E-m_N-\Sigma^{(1)}(E)]^{-1} \ , \tag{14}$$

$$\Sigma^{(1)}(E)=\Sigma^{(2)}+\langle f^{(2)}|G_0(E)|f^{(1)}\rangle \ , \tag{15}$$

where we have explicitly shown the energy dependence of all quantities for two-body unitarity to be satisfied. In particular, we observe that the $\pi NN$ vertex $|f^{(1)}(E)\rangle$ does not only depend on the momentum but has energy dependence, and this energy dependence arises from dressing [second term on the right-hand side of Eq. (12)]. Also the nucleon propagator $g(E)$ has dressing included through $\Sigma^{(1)}(E)$. The dressing in both the $\pi NN$ vertex and nucleon propagator is the minimum required for two-body unitarity to be satisfied.[14] For this reason we do not have any nonlinearity in our equations.

The above result has been shown to be equivalent to the solution of the two-body equation (e.g., the Lippmann-Schwinger equation) for the energy dependent two term separable potential[14]

$$V=|h\rangle\lambda\langle h| + |f^{(2)}\rangle\frac{1}{E-m_0}\langle f^{(2)}| \ , \tag{16}$$

where

$$m_0=m_N+\delta m \tag{17}$$

with $\delta m=\Sigma^{(2)}$ playing the role of a mass counter term.

Although we have included the minimum dressing to satisfy two-body unitarity, we need to guarantee that our nucleon propagator $g(E)$ has the correct asymptotic limit. In particular $g(E)$ should have a simple pole at $E=m_N$ and the residue of $g(E)$ at this pole should be one.[15] In other words, on the mass shell the nucleon propagator $g(E)$ should reduce to the free propagator $g_0(E)$. To satisfy these two conditions we write

$$\Sigma^{(1)}(E)=\delta m+\Gamma(E) \ , \tag{18}$$

where $\delta m=\Sigma^{(2)}$. The mass counter term can be taken as a constant. Using the fact that

$$G_0(E)=G_0(m_N)-(E-m_N)G_0(m_N)G_0(E) \ , \tag{19}$$

and

$$\tau(E)=\tau(m_N)-(E-m_N)\tau(m_N) \times\langle h|G_0(m_N)G_0(E)|h\rangle\tau(E) \ , \tag{20}$$

we can write

$$\Gamma(E)=\Gamma(m_N)-(E-m_N)\Gamma_1(m_N) +(E-m_N)^2\Gamma_2(E) \ . \tag{21}$$

We now can write Eq. (14) for the nucleon propagator as

$$g^{-1}(E)=(E-m_N)[1+\Gamma_1(m_N)-(E-m_N)\Gamma_2(E)] -\delta m-\Gamma(m_N) \ . \tag{22}$$

The condition that $g(E)$ has a simple pole at $E=m_N$ implies that

$$\delta m=-\Gamma(m_N) =-\langle f^{(2)}|G_0(m_N)|f^{(1)}(m_N)\rangle \ . \tag{23}$$

To get a residue of one at $E=m_N$ we need to introduce a renormalized propagator $g_R(E)$ and a wave function renormalization constant $Z_2$ such that

$$g^{-1}(E)=[1+\Gamma_1(m_N)](E-m_N) \times\left[1-\frac{(E-m_N)\Gamma_2(E)}{1+\Gamma_1(m_N)}\right] \equiv Z_2{}^{-1}g_R{}^{-1}(E) \ , \tag{24}$$

where

$$Z_2=[1+\Gamma_1(m_N)]^{-1} \ . \tag{25}$$

We now can write the $\pi$-$N$ amplitude given by Eq. (11) in terms of renormalized nucleon propagator and $\pi NN$ vertex as

$$t(E)=|h\rangle\tau(E)\langle h| + |f_R^{(1)}(E)\rangle g_R(E)\langle f_R^{(1)}(E)| \ , \tag{26}$$

where

$$\begin{aligned}|f_R^{(1)}(E)\rangle &= |f^{(1)}(E)\rangle Z_2^{1/2} \\ &= |f_R^{(2)}\rangle \\ &\quad + |h\rangle\tau(E)\langle h|G_0(E)|f_R^{(2)}\rangle \ ,\end{aligned} \tag{27}$$

with

$$|f_R^{(2)}\rangle = |f^{(2)}\rangle Z_2^{1/2} \ . \tag{28}$$

The dressed renormalized nucleon propagator can now be written as

$$g_R^{-1}(E)=(E-m_N)[1-(E-m_N)\Gamma_2^R(E)] \ , \tag{29}$$

where

$$\begin{aligned}\Gamma_2^R(E) &= Z_2\Gamma_2(E) \\ &= \langle f_R^{(1)}(m_N)|G_0{}^2(m_N)G_0(E)|f_R^{(1)}(E)\rangle \\ &\quad + \langle f_R^{(1)}(m_N)|G_0{}^2(m_N)|h\rangle\tau(m_N) \\ &\quad \times\langle h|G_0(m_N)G_0(E)|f_R^{(1)}(E)\rangle \ .\end{aligned} \tag{30}$$

Finally, we can write the wave function renormalization constant $Z_2$ in terms of the renormalized $\pi NN$ vertex as

$$Z_2=1-\Gamma_1^R(m_N) \ , \tag{31}$$

where

$$\begin{aligned}\Gamma_1^R(m_N) &= Z_2\Gamma_1(m_N) \\ &= \langle f_R^{(1)}(m_N)|G_0{}^2(m_N)|f_R^{(1)}(m_N)\rangle \ .\end{aligned} \tag{32}$$

Although $\Gamma_1^R(m_N)>0$, we will find that $Z_2>0$ from our numerical calculation. This is consistent with Eq. (25) which gives a positive value for $Z_2$.

## III. NUMERICAL RESULTS

It is a well known fact that the $\pi$-$N$ amplitude in the $P_{11}$ channel becomes highly inelastic above the threshold for pion production. Furthermore, the phase shifts, which are small and negative for $T_\pi^{\text{lab}}<150$ MeV, go through 90° at a pion energy of $T_\pi^{\text{lab}}=530$ MeV, indicating the presence of the well known Roper resonance [$N^*(1470)$]. However, since most pion-nucleus experiments are below the threshold for single pion production, we have chosen to neglect the effect of inelasticity in our present parametrization of the $P_{11}$ amplitude. On the other hand, the Roper resonance can be due to a resonance in $t_{\text{np}}$ which is shifted to higher energies in the full amplitude. In the Appendix we show how this shift arises in the present model. Since $t_{\text{np}}$ is that part of the $\pi$-$N$ amplitude which gives rise to pion multiple scattering in nuclei, a resonance in this amplitude can have drastic effects on the pion-nucleus amplitude. Furthermore, a resonance in $t_{\text{np}}$ leads to a resonance behavior in the dressed $\pi NN$ form factor [see Eq. (12)] which in turn can greatly influence the pion absorption cross section.

To study the effect of a resonance in $t_{\text{np}}$ on the $\pi NN$ vertex $f^{(1)}$ and nucleon propagator $g$, we have constructed two parametrizations of the $\pi$-$N$ amplitude that fit the scattering length and low energy ($T_\pi^{\text{lab}}<300$ MeV) phase shifts. In this way we hope to study the role of such resonances in $\pi$-$d$ elastic scattering and pion absorption. To construct our $\pi$-$N$ amplitudes we need to specify the undressed $\pi NN$ form factor $f^{(2)}(p)$ and the form factor for the separable non-pole part of the potential $h(p)$. In the present investigation we choose these to be

$$h(p)=c\frac{p}{p^2+\beta^2} \ , \tag{33}$$

$$f^{(2)}(p)=a\frac{p}{(p^2+d^2)^2} \ . \tag{34}$$

In this way we have four parameters $(c,\beta,a,d)$ to fit the experimental data. In Table I we present the parameters of our two fits; included also are the $\pi$-$N$ scattering length, the $\pi NN$ coupling constant, and the wave function renormalization $Z_2$. Here the $\pi NN$ coupling constant was determined by the direct comparison of the residue of our amplitude with that of the invariant amplitude for the nucleon pole diagram. The parameter set A (set B) leads to a resonance (no resonance) in $t_{\text{np}}$. For comparison with the standard energy independent potential, we will compare our parametrization with that of Blankleider and Afnan (potential $B\phi8$) (Ref. 7) which will label as set C.

In Fig. 3 we compare the phase shifts for the three parametrizations with the experiment. We find that all three parametrizations fit the scattering phase shifts very well below the pion production

TABLE I. The parameters of the $P_{11}$ amplitude for sets A and B. Included also are the prediction of the models for the scattering length, the $\pi NN$ coupling constant, and wave function renormalization. The experimental data are from Ref. 18.

| | Set A (resonance case) | Set B (nonresonance case) | Experiment |
|---|---|---|---|
| $\lambda$ | $-1$ | $-1$ | |
| $c$ | 1.00899 | 0.535314 | |
| $\beta$ | 5.05533 $\text{fm}^{-1}$ | 1.24487 $\text{fm}^{-1}$ | |
| $a$ | 1.00489 $\text{fm}^{-5/2}$ | 8.44136 $\text{fm}^{-5/2}$ | |
| $d$ | 1.33725 $\text{fm}^{-1}$ | 2.19154 $\text{fm}^{-1}$ | |
| $a_s$ | $-0.0908$ $m_\pi^{-3}$ | $-0.0908$ $m_\pi^{-3}$ | $-0.0845\pm0.0102$ $m_\pi^{-3}$ |
| $f_{\pi NN}{}^2$ | 0.03576 | 0.08198 | $0.082\pm0.015$ |
| $Z_2$ | 0.9850 | 0.8626 | |

threshold ($T_\pi^{\text{lab}} < 300$ MeV). It is difficult to compare our phase shifts with the experiment above the production threshold since we have not included inelasticity. However, we observe that the phase shifts for case A, which has a resonance in $t_{\text{np}}$, tend toward 90° at high energies, while the phase shifts for sets B and C parametrization agree with each other and fail to approach 90°.

To examine the relative contribution of the pole and non-pole amplitudes, we present in Figs. 4 and 5 the phase shifts corresponding to $t_{\text{np}}$ and $t_{\text{pole}}+t_{\text{np}}$ for both sets A and B. We find that for both sets A and B the non-pole part of the amplitude is attractive and large. This implies that the small experimental phase shifts are the result of a cancellation between two large amplitudes. The significant implication of this result, regarding pion-nucleus scattering, is that the two parts of the amplitude are weighted differently. Thus, $t_{\text{np}}$, which enters on an equal footing with all the other $\pi$-$N$ amplitudes, gives rise to pion multiple scattering. On the other hand, $t_{\text{pole}}$ gives us the $\pi NN$ form factor and thus determines the role of real pion absorption in pion elastic scattering. Although we have almost total cancellation in the $\pi$-$N$ system for $T_\pi^{\text{lab}} < 150$ MeV, the effect is more pronounced in $\pi$-$d$ scattering[1,7] and presumably in pion scattering off heavier nuclei.

To examine more closely the relative magnitude of the pole and non-pole amplitudes, we present in Figs. 6 and 7 the ratio of $\text{Re}(t_{\text{np}})/\text{Re}(t_{\text{pole}})$ and $\text{Im}(t_{\text{np}})/\text{Im}(t_{\text{pole}})$ for the three different parametrizations being considered. We find that for sets B and C the pole and non-pole amplitude are close in magnitude but opposite in sign. Furthermore, the

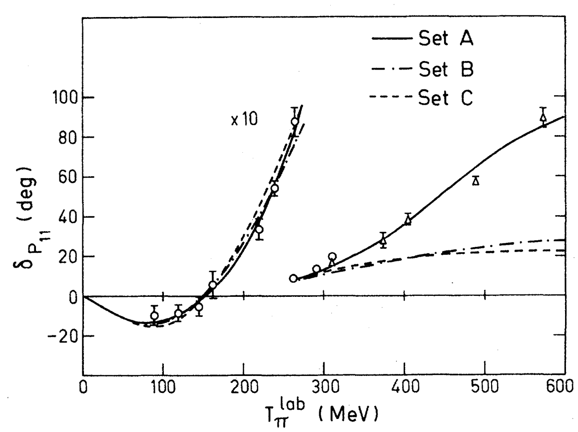


FIG. 3. The $P_{11}$ phase shifts for the three different parametrizations: —— the results for set A; —·—·—· the results for set B; and — — — the results for set C. The circles (Φ) are the experimental points from Ref. 16, while the triangles (Δ) are from Ref. 17.

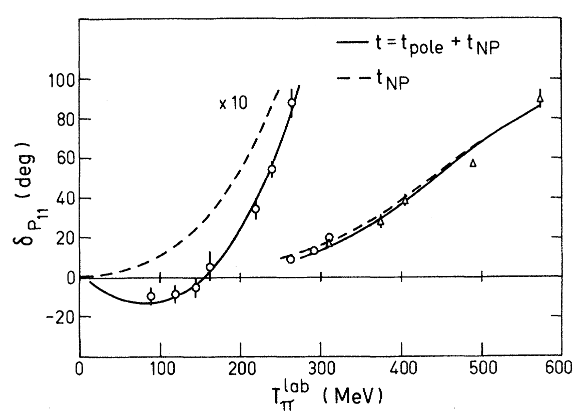


FIG. 4. The $P_{11}$ phase shifts for parameter set A: — — — represent the phase shifts for $t_{\text{np}}$, while —— are the phase shifts for the full amplitude. The experimental points are as in Fig. 3.

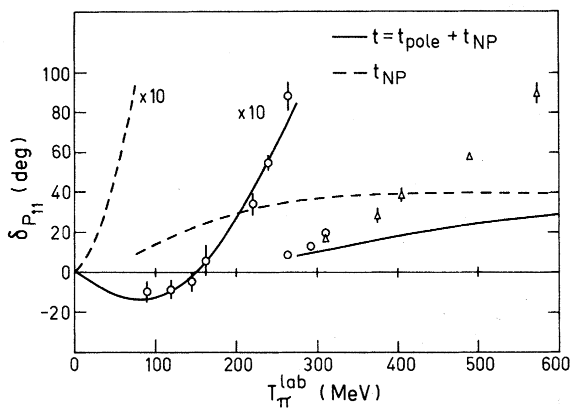


FIG. 5. The $P_{11}$ phase shifts for parameter set B; the labeling is as in Fig. 4.

potential approach of Blankleider and Afnan (set C) (Ref. 7) gives results that are similar to those of set B which has no resonance in $t_{np}$. On the other hand, for the case when $t_{np}$ has a resonance (set A) the pole and non-pole amplitude are quite different in that the $\mathrm{Im}(t_{pole})$ has a zero at $T_\pi^{lab} \simeq 100$ MeV, and at high energies the $t_{np}$ is much larger than $t_{pole}$. This difference between the two parametrizations (sets A and B) can give different results in pion-nucleus calculations. This can be further illustrated by comparing the amplitudes for the three

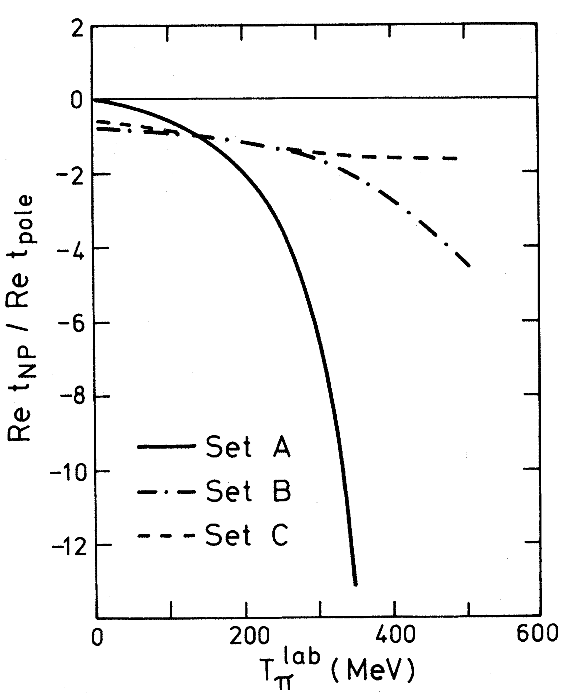


FIG. 6. The ratio of $\mathrm{Re}(t_{np})/\mathrm{Re}(t_{pole})$ for the on-shell amplitudes. The curves are labeled as in Fig. 3.

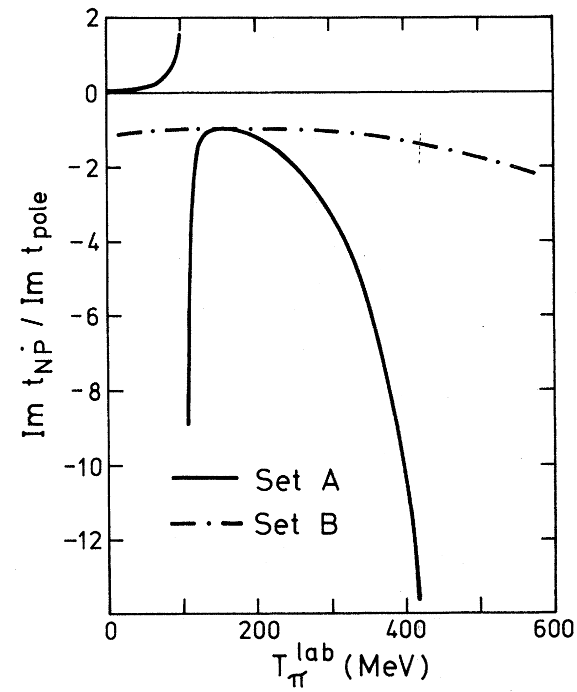


FIG. 7. The ratio of $\mathrm{Im}(t_{np})/\mathrm{Im}(t_{pole})$ for the on-shell amplitudes. The curves are labeled as in Fig. 3.

parametrizations off the energy shell at negative energies. For it is these amplitudes that are the input to Faddeev-type calculations. In Figs. 8 and 9 we give the ratio $(t_{np}/t_{pole})$ half off-shell for center-of-mass energies of $-43$ and $-200$ MeV. Here again we observe the similarity of the amplitudes for sets B and C with no resonance in $t_{np}$, while set A has quite distinct off-shell behavior.

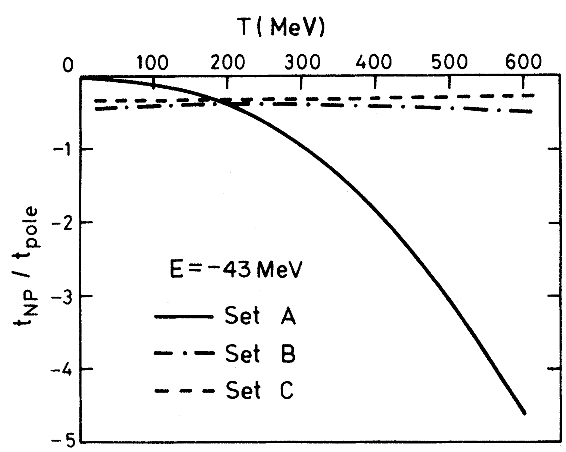


FIG. 8. The ratio of $t_{np}$ to $t_{pole}$ for center-of-mass energy $E = -43$ MeV. The momenta correspond to the pion laboratory energy $T$. The curves are labeled as in Fig. 3.

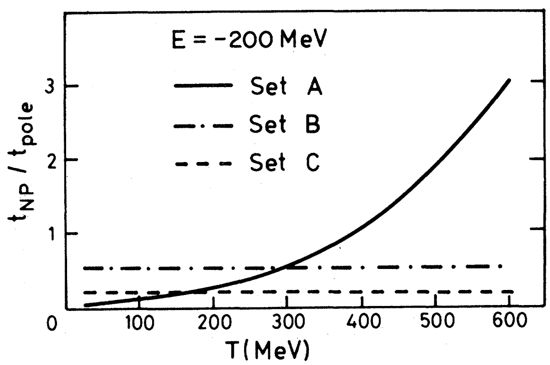


FIG. 9. The ratio of $t_{np}$ to $t_{pole}$ for center-of-mass energy $E = -200$ MeV. See the caption of Fig. 8.

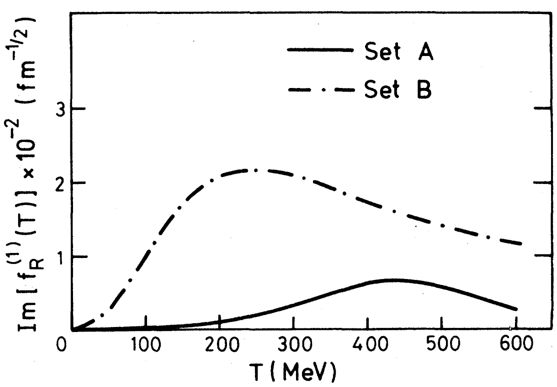


FIG. 11. The imaginary part of the dressed $\pi NN$ factor. See the caption of Fig. 10.

Finally we turn to the dressed $\pi NN$ form factor which in this case is energy dependent, and the nucleon propagator. In Figs. 10 and 11 we present the real and imaginary part of $f_R^{(1)}$. We note that for the potential model of Blankleider and Afnan (set C) (Ref. 7) the $\pi NN$ form factor is a real function. The fact that the imaginary part of $f_R^{(1)}$ is an order of magnitude smaller than the real part may be considered as a justification for the use of simple potential models. A comparison of the range of the $\pi NN$ form factor for the different models reveals that in general this formulation gives a much longer (shorter) range form factor in coordinate (momentum) space than is usually assumed. This may be a consequence of the choice of form factors in Eqs. (33) and (34). We also observe that the form factor for set B is larger than is the case for set A. Turning to the dressed propagator given in Figs. 12 and 13 we find that the dressed propagator for set A is closer to the result of Blankleider and Afnan (set C) (Ref. 7) than is the case for set B. This is reflected in the fact that the wave function renormalization constant $Z_2$ is closer to one for set A than is the case for set B (see Table I). In other words, the effect of dressing is not as important.

We have thus demonstrated that a fit to the $P_{11}$ phase shifts does not uniquely determine the off-shell $P_{11}$ amplitude. More important we have seen that the relative magnitude of the pole and non-pole parts of the amplitude cannot be determined on the basis of the experimental $\pi$-$N$ phase shifts. In particular, the inclusion of a resonance in $t_{np}$ can render quite a different result for both the $\pi NN$ form factor and the relative magnitude of $t_{pole}$ and $t_{np}$. This uncertainty should be resolved before one can predict any unique result for the $\pi NN$ system

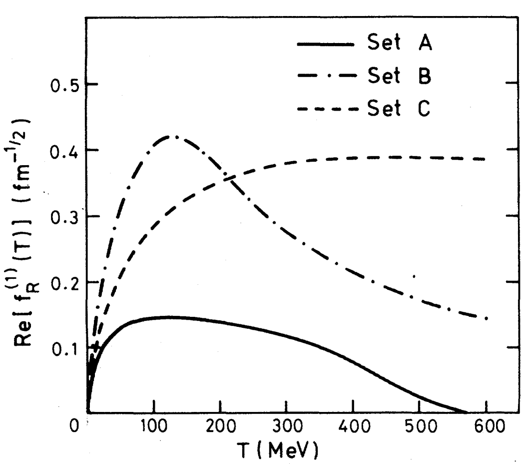


FIG. 10. The real part of the dressed $\pi NN$ form factor. The energy $T$ is the pion laboratory energy. Curves labeled as in Fig. 3.

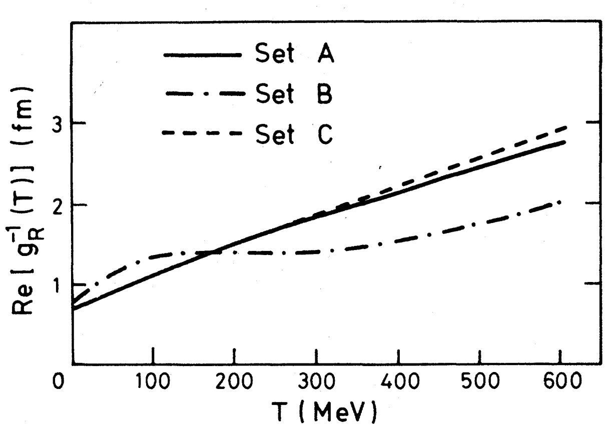


FIG. 12. The real part of the dressed propagator. For parameter set C we have no dressing of the propagator. See the caption of Fig. 10.

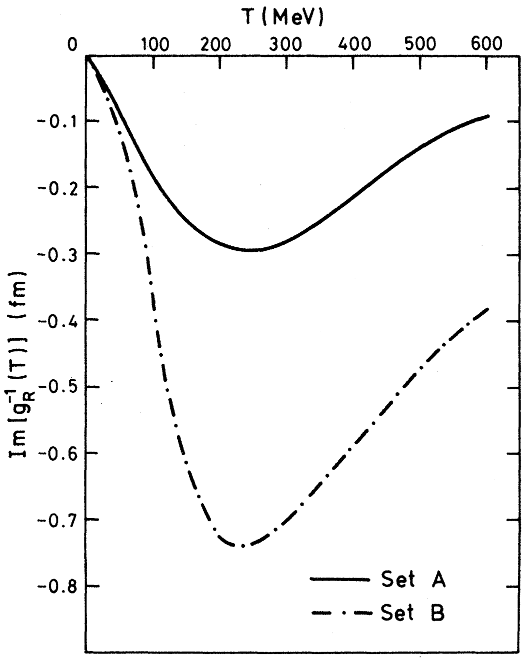


FIG. 13. The imaginary part of the dressed propagator. See the caption of Fig. 10.

with the present form for the $\pi$-$N$ amplitudes in the $P_{11}$ channel.

## ACKNOWLEDGMENTS

The authors would like to acknowledge many useful discussions with Dr. B. Blankleider, Dr. R. T. Janus, Dr. A. T. Stelbovics, and Mr. J. McCarthy. One of us (S.M.) is grateful to the Australian Research Grants Committee for a research fellowship.

## APPENDIX

In this appendix we show that a resonance pole in $t_{np}$ is shifted in energy in $t = t_{pole} + t_{np}$. Our proof is based on the equivalence between the results of Eqs. (2)–(4) and the amplitude for a two term separable potential of the form[14]

$$V(E) = |f^{(2)}\rangle \frac{1}{E-m_0}\langle f^{(2)}| + |h\rangle\lambda\langle h| \equiv v_1(E) + v_2 \ . \tag{A1}$$

The non-pole part of the amplitude is a solution of Eq. (3) with $t^{(2)} = v_2$. Since $v_2$ is separable we can write $t_{np}(E)$ as

$$t_{np}(E) = |h\rangle \tau_{np}(E) \langle h| \tag{A2}$$

with

$$\tau_{np}(E) = (\lambda^{-1} - \langle h | G_0(E) | h\rangle)^{-1} \ . \tag{A3}$$

The existence of a resonance pole at $E = E_R$ implies that

$$\tau_{np}{}^{-1}(E)\,|_{E=E_R} = 0 \ , \tag{A4}$$

or

$$\lambda^{-1} = \langle h | G_0(E_R) | h\rangle \ . \tag{A5}$$

This allows us to write Eq. (A3) as

$$\tau_{np}(E) = \frac{F(E)}{E-E_R} \ , \tag{A6}$$

with

$$F(E) = \langle h | G_0(E_R) G_0(E) | h\rangle \ . \tag{A7}$$

In writing Eq. (A6) we have made use of a relation similar to that of Eq. (19). The full amplitude can now be written as

$$t(E) = t_{np}(E) + |f^{(1)}(E)\rangle g(E) \langle f^{(1)}(E)| \ , \tag{A8}$$

where the dressed $\pi NN$ form factor given in Eq. (12) has the resonance pole which can explicitly be exposed to give

$$|f^{(1)}(E)\rangle = \frac{1}{E-E_R}[(E-E_R)|f^{(2)}\rangle + |h\rangle F(E) \langle h | G_0(E) | f^{(2)}\rangle] \ . \tag{A9}$$

However, this pole in $f^{(1)}(E)$ does not lead to a second order pole in the amplitude since the dressed propagator has a zero at $E = E_R$ which can be exposed to give

$$g(E) = [E - m_0 - \Gamma(E)]^{-1} = -\frac{(E-E_R)}{D(E)} \tag{A10}$$

with

$$D(E)=d(E)-(E-E_R)[E-m_0-G_{11}(E)] \quad \text{(A11)}$$

and

$$d(E)=G_{12}(E)F(E)G_{21}(E)\ . \quad \text{(A12)}$$

Here the $G_{ij}(E)$ are given by

$$\begin{aligned} G_{11}(E)&=\langle f^{(2)} \mid G_0(E) \mid f^{(2)}\rangle\ ,\\ G_{21}(E)&=\langle h \mid G_0(E) \mid f^{(2)}\rangle\ ,\\ G_{12}(E)&=\langle f^{(2)} \mid G_0(E) \mid h\rangle\ . \end{aligned} \quad \text{(A13)}$$

We thus see that any resonance pole in $t_{\rm np}$ will also be in $t_{\rm pole}$ with opposite sign which might lead to the cancellation of the resonance pole in the full amplitude. We will now show that in fact the full amplitude does not have a resonance pole at $E=E_R$, but has a pole at $E=E_R+\Delta$ where $\Delta$ is a complex number. To see this we substitute the results of Eqs. (A9) and (A10) in Eq. (A8) to get for the full amplitude

$$\begin{aligned} t(E)=&\mid h\rangle F(E)\left[E-E_R-\frac{d(E)}{E-m_0-G_{11}(E)}\right]^{-1}\langle h \mid\\ &-\mid f^{(2)}\rangle\frac{E-E_R}{D(E)}\langle f^{(2)}\mid\\ &-\mid f^{(2)}\rangle\frac{G_{21}(E)F(E)}{D(E)}\langle h\mid\\ &-\mid h\rangle\frac{F(E)G_{12}(E)}{D(E)}\langle f^{(2)}\mid\ . \end{aligned} \quad \text{(A14)}$$

This amplitude has a pole at

$$E=E_R+\frac{d(E)}{E-m_0-G_{11}(E)}$$

and this pole can be a resonance pole.

---

*Present address: Department of Physics, Purdue University, West Lafayette, Indiana 47907.


[1]I. R. Afnan and B. Blankleider, Phys. Lett. 93B, 367 (1980).

[2]C. Fayard, G. H. Lamot, and T. Mizutani, Phys. Rev. Lett. 45, 524 (1980).

[3]D. S. Koltun and T. Mizutani, Phys. Rev. C 22, 1657 (1980).

[4]Y. Avishai and T. Mizutani, Phys. Rev. C 22, 2492 (1980).

[5]A. W. Thomas and R. H. Landau, Phys. Rep. 58, 121 (1980).

[6]N. Giroud, C. Fayard, and G. H. Lamot, Phys. Rev. C 21, 1959 (1980).

[7]B. Blankleider and I. R. Afnan, Phys. Rev. C 24, 1572 (1981).

[8]J. G. Taylor, Nuovo Cimento, Suppl. 1, 857 (1963); Phys. Rev. 150, 1321 (1966).

[9]T. Mizutani and D. S. Koltun, Ann. Phys. (N.Y.) 109, 1 (1977).

[10]I. R. Afnan and B. Blankleider, Phys. Rev. C 22, 1638 (1980).

[11]Y. Avishai and T. Mizutani, Nucl. Phys. A338, 377 (1980).

[12]A. W. Thomas, Nucl. Phys. A258, 417 (1976).

[13]S. Théberge, A. W. Thomas, and G. A. Miller, Phys. Rev. D 22, 2838 (1980).

[14]I. R. Afnan and A. T. Stelbovics, Phys. Rev. C 23, 1384 (1981).

[15]W. M. Kloet and R. R. Silbar, Nucl. Phys. A338, 281 (1980).

[16]J. R. Carter, D. V. Bugg, and A. A. Carter, Nucl. Phys. B58, 378 (1973).

[17]P. Bareyre, C. Brickman, A. V. Stirling, and G. Villet, Phys. Lett. 18, 342 (1965).

[18]V. K. Samaranayake and W. S. Woolcock, Nucl. Phys. B49, 128 (1972); V. Haber-Schaim, Phys. Rev. 104, 1113 (1956).